SLS-TME-TA-1998-0011
September 15, 1998

RF system for the SLS Booster and Storage Ring

Patrick Marchand

PSI

Contents:

RF System for the SLS Booster and Storage Ring

1. Introduction

The RF system for the SLS storage ring has a double task: compensating for the beam energy losses due to synchrotron radiation and providing the accelerating voltage necessary to achieve the required momentum acceptance. Several alternative versions have been considered and compared [1,2]. The solution which was adopted for the starting phase is based on the use of conventional, already well-proven equipment that should be available and operational within relatively short times, compatible with the SLS schedule. It consists of four 500 MHz plants, each comprising a normal conducting (nc) single-cell cavity of the ELETTRA type, powered with a 180 kW CW klystron amplifier via a WR1800 waveguide line.
In spite of the lower power requirement, one similar plant will be used for the booster with the intention of standardising.
The cavities with their input couplers, their tuning and cooling systems as well as the phase and amplitude regulation loops will be supplied by Sincrotone Trieste, the klystrons by EEV Ltd, the klystron supplies and control systems by THOMCAST AG.
The use of superconducting (sc) cavities has been ruled out as a starting solution. However, combining "HOM free" sc cavities with the initial nc system is regarded as a possible future option for improving the beam lifetime in the storage ring when operating at very high brightness. Either the energy acceptance could be increased using one 500 MHz sc cavity [3,4], or the bunches could be lengthened using one (possibly two) higher harmonic sc cavity(ies) [5]. Within both schemes, the sc cavities could be operated in an entirely idle mode (no external RF source). A more detailed description of this possible further upgrading is reported in [6].

2. Design parameters

The basic parameters of the storage ring [7] which affect the RF system are listed in the upper part of Table 1.
The selection of the RF frequency was mainly dictated by the availability of commercial RF power sources and other components. We chose 500 MHz, the mostly used frequency. Moreover, it is a good compromise as regard to the equipment size, the required RF voltage and power as well as the corresponding bunch length. These quantities are related to the storage ring parameters as follows:

$$eV_{RF} = q\,\Delta U = \Delta U / \sin\phi_s;$$
$$\varepsilon_{RF} = [F(q)\,\Delta U / (\pi\,\alpha\,h\,E)]^{1/2}, \text{ where } F(q) = 2\,[(q^2 - 1)^{1/2} - \arccos(1/q)];$$
$$\sigma_s = c\,\alpha\,\sigma_p / (2\,\pi\,f_s), \text{ where } f_s = f_{RF}\,[\alpha\,V_{RF}\cos\phi_s / (2\,\pi\,h\,E/e)]^{1/2};$$
$$P_b = I_b\,\Delta U/e.$$

The definition of the notations used above as well as numerical values for the SLS are given in Table 1. The total RF power requirement, P_{RF} is then determined by the number of RF cavities, n_c and their shunt impedance, R_s:

$$P_{RF} = P_b + P_d,$$
where $P_d = V_{RF}^2 / (2\,n_c\,R_s)$ is the cavity wall dissipation.

We assumed here that the system was matched (zero reflected power) at full beam current. This condition which minimizes the maximum power requirement is fulfilled only if:

- the reactive component of the beam current is canceled by properly detuning the cavity so that the beam-loaded cavity is "seen" as a pure resistance;
- this equivalent resistance is matched to the RF source impedance by a correct setting of the coupling factor.

The detuning, Δf_m and the coupling factor, β_m satisfying these two conditions are given by:

$$\Delta f_m = (f_{RF} / 2 Q_o) (P_b / P_d) \cot g \phi_s ,$$

$$\beta_m = 1 + (P_b / P_d) ,$$

where Q_o is the unloaded cavity quality factor.

3. RF cavities and associated equipment

3.1 RF cavities

Four nc single-cell cavities of the ELETTRA type will provide the required RF voltage and power. They will be manufactured from high purity (99.99 %), high conductivity (HC), oxygen-free (OF) seamless copper forging and equipped with 8 equatorial outlet ports: 3 large ones - for the input power coupler, the pumping system, the plunger tuner - and 5 smaller ones for vacuum and RF monitoring. The cavity shape is shown in Figure 1 and its main performance data are listed in Table 2 [8].

The parameter values in Table 3 show that, using four such cavities, the RF system has the potential for achieving the SLS requirement with a cavity input power lower than 150 kW. Besides, would one of the four cavities be out of use, the operation at full beam current is still possible with an RF voltage of about 2 MV.

The cavities will be accommodated in pairs in two of the dispersion free, low β, 4 m long straight sections of the storage ring (SS2 and SS8), as shown in Figure 2.

Values of shunt impedance 20 - 30 % larger could be obtained with nose cone (re-entrant) cavities [9-14], leading to a total power savings of about 10 %. Nevertheless, we selected the "elliptical" shape which is less susceptible to multipactor, and makes easier the cooling and manufacturing. Due to the relatively high beam power, low RF voltage and the practical limitations for the input couplers, the interest of multicell or sc cavities is rather limited here. Moreover the use of single cell cavities minimizes the number of Higher Order Modes (HOM) that could drive coupled bunch instabilities (see section 7).

3.2 Input couplers

The input coupler must be capable to feed into the cavity a CW RF power of at least 150 kW (forward) and also to handle the full reflection. It will be similar to those operating in ELETTRA which are of the coaxial type, terminated by a coupling loop. The air to vacuum transition is ensured by a cylindrical ceramic window brazed inside the coaxial line. Although the operating power at ELETTRA does not exceed 65 kW, the same coupler has successfully been tested up to 330 kW at DESY [15] and therefore should be capable to fulfil the SLS requirement. The coupling coefficient shall be adjustable within a range of 1 to 3.5 in order to match different beam loading conditions.

The coupler will be mounted on one of the three large cavity equatorial ports and connected to the WR1800 waveguide line by means of a standard 6-1/8" waveguide-to-coaxial transition (see Figure 2).

3.3 Cooling systems

The cavities are cooled by means of water flowing through pipes, brazed into channels which are machined around the cavity outer surface and outlet ports, as shown in Figure 1. This cooling circuit must be able to remove up to 65 kW of power dissipation into the cavity wall. In addition, it shall be possible - thanks to the cooling system - to set the cavity temperature at any value within 60 ± 25 °C with a stability of ± 0.05 °C (for $0 \leq Vacc \leq 650$ kV). This is achieved by properly isolating the cavity and by re-circulating the cooling water through an appropriate heat exchanger water station (cooling rack) dedicated to each cavity. The cavity temperature is measured by a thermocouple, compared to a reference value and the error signal used for regulation in the cooling rack. Controlling the cavity operating temperature within the above specified range shall prevent coupled bunch instabilities with a beam current up to 400 mA (see section 7).

3.4 Frequency tuning systems

As mentioned before the HOM frequencies will be controlled by proper setting of the cavity water cooling temperature. A plunger tuner, installed on one of the three large cavity equatorial ports, shall provide an additional degree of freedom in tuning the fundamental and HOM frequencies.
The proper adjustment of the fundamental frequency for variable beam loading - with different operating temperatures and plunger positions - will be performed by means of a mechanical system driven with a stepping motor which will change the cavity length (longitudinal squeezing or stretching), within the range of elastic deformation. This system can provide a fundamental tuning range of ± 200 kHz. In operation, the cavities will be automatically tuned by a regulation loop (see section 5).

3.5 Other cavity associated equipment

Four of the five small cavity equatorial ports will be equipped with monitoring RF pick-ups, three loops and one antenna. The fifth one will be used for vacuum monitoring.
A prevacuum turbomolecular pump and a UHV ion pump (≥ 120 l/s) will be installed on one of the three large cavity equatorial ports. Pressures around $1.\ 10^{-9}$ mbar are expected with an accelerating voltage of 650 kV and a cavity wall temperature up to 85 °C.
For the bakeout of the cavities, the cooling water will be heated up to 150 °C by means of portable heater units. An appropriate insulating jacket will reduce heat exchange and ensure a tight thermal stability during the bakeout or power operations. A set of sixteen thermocouples will allow to map the temperature distribution on the cavity outer surface.

4. RF power source and feeder line

Each cavity will be individually powered with a CW klystron amplifier capable to deliver more than 180 kW. The klystrons whose main characteristics and performance are summarized in Table 4 will be provided by the firm EEV Ltd.
The klystron DC supplies for the cathode and auxiliaries (anode modulation, cathode heating, focal coils, ion pump) will be provided by the firm THOMCAST AG. The power supplies and the control system are hosted in three different cabinets which belong to a single mechanical unit, as described in Figure 3.
The DC power supply for the cathode is a Pulse Step Modulator (PSM) currently used for broadcast transmitters [16]. Conceptual electronic diagrams are shown in Figure 4. Designed for 46 kV - 7.5 A, this PSM essentially consists of 68 power modules which are connected in series and supplied through their own secondary winding from two transformers. The two transformers are shifted in phase, resulting in a 12-pulse loading of the mains with a 6-pulse rectification in the module chain. Each one of the 68 modules represents an autonomous

voltage source (Us ≈ 730 V) which may be switched on/off individually by means of fast IGBT switches operating at 14 kHz. The switching sequence and pulse duration is generated and supervised by the PSM control system such that the thermal loading of all modules is distributed equally. The switching frequency can be suppressed at the output of the module chain, by means of a low pass filter.
The main PSM features (efficiency, regulation speed and accuracy, compatibility with large variation of the load impedance) well comply with the performance specifications which are listed in Table 5. Moreover, the modular concept with high redundancy (up to four defective modules without performance degradation) makes it very reliable, easy to maintain and there is no need for HV crowbars.
The RF power delivered by the klystron will be fed into the cavity input coupler via a WR1800 waveguide line including monitoring directional couplers as well as a circulator to isolate the klystron from the variable (beam-loaded) cavity impedance. All these waveguide components are commercially available. The four RF plants of the SR are arranged in pairs in two diagonally opposite RF stations. Figure 5 shows a layout of one of them.

5. Variable beam loading compensation and low level electronic system

5.1 Variable beam loading compensation

Until now we assumed a steady state regime and a matching condition at full beam current ($\Delta f = \Delta f_m$ and $\beta = \beta_m$). Numerical values of Δf_m and β_m for the SLS typical operating conditions are given in Table 3. While filling the storage ring, the beam loading is varying. Maintaining the reactive beam loading compensation at constant RF voltage essentially requires the use of two servo loops:

- *the frequency tuning loop* (or "slow" phase loop) which must keep constant the phase of the RF voltage in tuning the cavity fundamental frequency;
- *the amplitude regulation loop* whose task consists in regulating the cavity input power to maintain the RF voltage constant.

Generally, *a "fast" phase loop* is also needed for compensating the phase changes which result from the varying power in the amplification chain.
Since during injection the coupling factor - whose variation would not be technically easy to realize - is kept constant and equal to β_m, there will be unavoidably some reflected power. Thanks to the circulator this reflected power, P_r will be directed to a dummy load and therefore not "seen" by the klystron. Figure 6 shows the variations of P_d, P_b, P_r and P_t for one cavity during the injection at 2.4 GeV.
When the above conditions are met, Robinson's criterion of stability for the fundamental mode is always fulfilled [17]. Figure 7 shows a stability diagram for the SLS at nominal performance. One can see that the stability margin is quite comfortable. As usual, the cavity will be tuned slightly below the RF source frequency (~ 1 kHz) in order to insure a sufficient stability margin at low beam current.
The low level electronic system comprising the regulation loops mentioned before (frequency, amplitude and phase) as well as the amplifier drive chain and the RF signal measurement channels will be supplied by Sincrotrone Trieste. That will be based on the system operating in ELETTRA with minor modifications for the SLS purpose as described below.

5.2 Fundamental frequency tuning loop

The tuning loop must adjust the fundamental resonant frequency to compensate the change in temperature and reactive beam loading (resistive impedance "seen" by the RF generator for any beam loading current). This is achieved in changing the cavity length within the elastic

deformation range by means of a mechanical system, driven by a stepping motor which longitudinally squeezes or stretches the cavity (symmetrical deformation).
A simplified block diagram of the loop is shown in Figure 8. The stepping motor is controlled in closed loop with the output signal from a phase detector; this signal is proportional to the phase difference between the cavity input signal (from waveguide directional coupler, WGC2) and the cavity pick-up signal (PU1). The phase shifter in the loop path provides an adjustable offset. Appropriate control and interlocks protect the cavity from exceeding the elastic deformation range. Besides, an input for an external interlock that can inhibit the tuning action, an output for external interlock purposes and the options of operating in open loop with local and remote control of the motor are also provided.
The main performance specifications are the following:

- tuning range : ± 200 kHz;
- tuning speed : adjustable up to 1 kHz / s;
- sensitivity : adjustable between ± 100 Hz and ± 1 kHz.

A tuning range of ± 200 kHz corresponds to a change in cavity length of ± 0.2 mm which remains in the limit of elastic deformation; it allows to handle cavity temperature variations of about ± 20 °C with a sufficient margin for the compensation of the largest beam loading effect which is less than 35 kHz (see Table 3). The tuning speed of 1 kHz/s is fast enough for the expected injection rates and the sensitivity of the loop will be experimentally optimised such that to avoid undue wear of the tuner.

5.3 Amplitude regulation loop

The amplitude loop must regulate the cavity accelerating voltage by controlling the drive power. A simplified block diagram of the loop is shown in Figure 9. A sample of the cavity voltage (from cavity pick-up, PU2) is detected and compared to the reference value; the error signal from the amplitude comparator is used to control a variable phase-free attenuator which sets the driving power. The “RF kick-off” input will be used to disable the loop during short RF interruptions that could be requested by the operator or the interlock system to dump the beam. The options for operating in open and closed loop, with local and remote control of the cavity voltage, are provided.
Modulating the klystron anode voltage - instead of the drive power - is regarded as another possible scheme of amplitude regulation. A switch is therefore implemented, as shown in Figure 9, in order to quickly change (during shutdown) the amplitude control mode, from drive to anode modulation, with direct setting of the drive level.
The main performance specifications are the following:

- open loop 3 dB bandwidth : adjustable up to 5 kHz;
- open loop DC gain : > 30 dB;
- output voltage stability : better than 1 %;
- recovery time (100 % modulation) : < 10 ms;
- output power dynamic : > 20 dB.

5.4 Phase regulation loop

The phase loop must compensate for the phase changes in the amplification chain with variable power. It shall also cope with the ripple coming from the klystron power supply.
A simplified block diagram of the loop is shown in Figure 10. The RF signals at the input and output of the amplification chain are compared in phase and the error signal is used to control an electronic phase shifter. PHS0 and PHS1 are mechanical phase shifters, driven with locally/remotely controlled motors; their variation range is 500° in steps of less than 1°. PHS1 is used to properly set the regulation point for any klystron operating conditions, while the reference phase of the plant is fixed by means of PHS0. The options for switching from open to closed loop and for disabling the loop action with an external interlock are provided.

The main performance specifications are the following:

- open loop 3 dB bandwidth : adjustable up to 5 kHz;
- open loop DC gain : > 30 dB;
- correction range : ± 30 °;
- phase stability : ± 0.5 °;
- recovery time (± 30 ° modulation): < 10 ms;
- output power dynamic : > 20 dB.

The bandwidth of both the phase and amplitude loops will be experimentally optimized to provide enough damping while remaining insensitive to the synchrotron frequency.
The combined performance of the power supplies, klystrons, phase and amplitude loops, as described before, should ensure highly stable conditions within the full SLS operating range of beam energy and current.

5.5 Drive chain

A simplified block diagram of the drive chain is shown in Figure 11. The signal from the 500 MHz master oscillator, after being split and phase/amplitude regulated, is amplified with a solid state 50 W drive amplifier.
A fast RF switch at the input of the chain can remove within less than 5 μs the driving RF signal under certain conditions (beam dump, klystron/cavity interlocks,…) and an output signal indicating the switch state is provided for interlock use.
A coaxial directional coupler monitors the RF signal right at the input of the klystron. The forward signal will be used to check the presence of drive power and also to protect the klystron against an overdrive. For this purpose, the rectified signal is compared to adjustable threshold values and then triggers the RF switch.
The whole drive chain shall have a 1 dB bandwidth of at least ± 10 MHz and input/output VSWR of less than 1.3 under any operating conditions.

5.6 RF signal measurements

As part of the low level electronics, measurement channels of RF signals picked up at different points of the system, are provided for monitoring purposes; they will be of three types: RF amplitude (or power), RF phase and direct RF measurements.
For the RF amplitude measurements, the rectified DC output voltage is 0 - 10 V and the accuracy better than 2 %.
For the RF phase measurements, the reference is the signal from the master oscillator. The DC output voltage is ± 10 V (for ± 180 °) and the accuracy better than 2 °.

6. RF control system

The RF control system will be produced in collaboration between THOMCAST and PSI. Its general task is to collect and process all the useful information coming from the various equipment parts in order to ensure a correct and safe (for personnel and equipment) operation of the RF system. A block diagram is shown in Figure 12.
The top level controller consists of a VME-bus crate operating under VxWorks and EPICS with an associated keypad and visual display. Its main functions are:

- local operator-machine interface;
- analog settings for the different equipment parts;
- command settings for the fast state machine;
- reading of the digital and analog signals;
- communication between the different VME stations (other RF plants and central SLS control system) for remote operation from the SLS main control room.

The control of the PSM is ensured by the PSM6C unit, a THOMCAST standard control and interface system which communicates with the PSM modules via fibre optic links.
The interlock protection system consists of a fast microcontroller (YCP16 from THOMCAST) and digital input/output printed circuit boards with programmable logic devices. The analog interlock inputs are converted into digital inputs by means of comparators with adjustable thresholds. The interlock state machine controls the starting-up and switching-off sequences of the various RF equipment parts. It is realised in YCP16 and each digital interlock input/output signal has its own logic programmed locally. In this logic, it is programmed under which condition the input has to cause a fallback of the state machine and the output (action) is processed as a function of the actual state. For each interlock input, three memories are used which store the first fault event, the status of all the signals at that time and the sequence of the faults occurring afterwards (up to 9 events). The fault event and status information is available in EPICS and also indicated on the front panel of the input/output printed circuit boards by means of two-colour LED's.
The different sub-units communicate via the control and interlock bus. The output voltage of the PSM and auxiliary supplies is set from EPICS by analog 0 - 10 V control signals. Fibre optical links are used for all control signals (readings and settings) at high potential and all the other input/output signals are galvanically isolated by means of optocouplers. The relevant analog and digital signals are also available on a connector panel for debugging purposes.
This system will be integrated in the SLS central control system for remote operation from the control room; nevertheless, it shall allow a stand-alone operation of each RF plant (independently of the SLS central system). It will be hosted in an EMC-shielded control cabinet and all electrical wiring made through a filter wall (see Figure 3).

7. Coping with the cavity HOM

As shown from the preceding results, the RF voltage and power requirement for the SLS remain relatively modest and can be achieved using conventional equipment. The main issue certainly resides in finding an efficient means of coping with the narrow band impedances of the cavity HOM which could drive Coupled Bunch Instabilities (CBI). Both types of CBI, longitudinal and transverse, can be generated by monopole and dipole modes respectively. When exciting a mode in resonance, the growth rate of the CBI is approximately given by:

$1 / \tau_{II} = I_b \, \alpha \, f_m \, R_{II} / (2 \, Q_s \, E/e)$ in the longitudinal case;

$1 / \tau_T = I_b \, \beta_T \, f_o \, R_T / (2 \, E/e)$ in the transverse case;

f_m : HOM frequency;

R_{II} and R_T : longitudinal [Ω] and transverse [Ω/m] HOM impedance;

$Q_s = f_s / f_o$: synchrotron tune; β_T : beta-function at the cavity location.

The stability is ensured when the growth rate of the CBI is less than the radiation damping rate. From the above formulas and the expected values of cavity HOM impedances [9,18,19], one can deduce that many of the HOM whose frequency is lower than the tube cutoff frequency are susceptible to generate CBI, limiting the maximum admissible current to levels as low as a few mA.
There exist different possible cures for this problem:

a) strong de-Qing of all the HOM resonances by means of external absorbers coupled to the cavities;
b) damping of the resulting oscillations by means of active feedback systems;
c) frequency tuning of the HOM resonances away from the coupled bunch modes spectral components;
d) creating artificial (Landau) damping, for instance with a higher harmonic RF system or by partial filling of the ring.

The efficiency of the last method is relatively limited and is regarded only as a complementary means of achieving the required stability.
Solution a) implies significant complications in the cavity design and fabrication. In order to fulfill the stability conditions, it is usually combined with b) which also requires rather complex components (broadband electronics, pick-ups, amplifiers and kickers). This is the approach followed for most of the future Meson Factories [20-23].
Solution c) which is already applied at several places, has been largely developed for the Tsukuba Photon Factory and recently improved by ELETTRA people [24]. In practice the HOM frequencies are controlled by temperature regulation of the cavity cooling water, while the fundamental mode is tuned by longitudinally squeezing/stretching the cavity. The installation of a plunger tuner provides an additional degree of freedom.
This technique of HOM tuning was preferred to the others, for the following reasons:

- it has been successfully experimented in ELETTRA with operating conditions very similar to ours;
- it does not require any special equipment on the cavities;
- it could be complemented - if necessary - by one of the methods mentioned before (a feedback system, for instance);
- it allows to switch at will between different modes of operation: a controlled excitation of the CBI is a way of trading off brightness for longer lifetime; this is applied in the "Elettra user mode" to increase the lifetime by a factor two at the expense of 20-30 % less brightness [25].

An illustration of this method, extrapolated to the SLS case, is shown in Figure 13. The measured longitudinal HOM parameters of one of the ELETTRA cavity, as listed in Table 6 [26], were used for the computation of the longitudinal CBI growth rates versus the cavity temperature. The horizontal axis crosses the vertical one at a point which corresponds to the radiation damping rate (~ 200 s^{-1}). Stability is insured when the growth rate is lower than this limit. The plot of Figure 13 shows that, within the temperature range of 40 - 70 °C, two large intervals fulfill this condition: 45 - 52 °C and 58.8 - 62 °C. Each peak represents the interaction of a HOM with a coupled bunch mode. It occurs three times - at a repetition of 1 MHz - for mode L9 which has the largest temperature coefficient and therefore determines the maximum width for a stable interval: 7.5 °C here. Modes L2, L6 and L8 are stable for any temperature while mode L1 would drive a CBI outside the operating range, at a temperature of 100 °C.
The fundamental frequency compensation for the beam loading does not dramatically modify the HOM distribution and only results in a reduction of the stable interval by a fraction of a degree.
It is worthwhile to note that this is a theoretical case, based on the use of a cavity which would be identical to the ELETTRA cavity considered here. Practically, due to the mechanical tolerances, the HOM distribution is different from one cavity to the other. *Although it is unlikely*, a configuration without any stable interval could be encountered for a specific cavity. This might happen, in particular, if mode L1 which has the largest impedance, the lowest temperature coefficient - and therefore exhibits the widest resonance - would fully interact within the operating temperature range. Such an unfavorable case, artificially created by proper modifying the HOM frequencies, is illustrated in Figure 14. As already mentioned, the use of a plunger aimed at shifting the frequency of mode L1 should prevent this kind of situation.
Applying the same treatment for the transverse dipole modes (Table 7) [26], we found that the situation was much less critical than in the longitudinal case. The stability is ensured provided that the horizontal and vertical β-functions at the cavity locations remain smaller than 0.5 m. Otherwise, resonant conditions should be easily avoidable by combining the HOM frequency control - as described before - with tune and chromaticity adjustments.

This method of dealing with the CBI requires a perfect knowledge of all the cavity mode parameters and their sensitivity to the different tuning means. A significant amount of theoretical and experimental work was performed in this domain at ELETTRA. The use of similar cavities and tuning devices for the SLS should permit to fully take advantage of this expertise.
The cavities, like any change in vacuum chamber cross section, also contribute to the ring effective broad band impedance, Z/n which leads to HOM power losses and can drive single bunch instabilities. A value of 1 Ω is considered as a reasonable guess for $(Z/n)_o$, the low frequency limit of Z/n [27]. We estimate the contribution of the four cavities to be about 10 %. The HOM power losses should not exceed a few kW for the entire ring and a few hundreds W in one cavity.

8. Booster RF system

Typical operating parameters of the booster [28] are listed in Table 8. Due to the lower beam current, the power requirement is significantly less than in the storage ring. However, with the intention of standardising we will use one 500 MHz plant similar to those of the storage ring. The major difference is that the RF power shall be cycled at 3 Hz by varying the reference voltage of the amplitude regulation loop as a function of the magnet field program. Contrary to the storage ring, the coupled bunch instabilities should not be an issue and therefore the cooling rack for the temperature control of the HOM frequencies is not needed. The cavity will be accommodated in one of the three booster straight sections and the RF station arranged as shown in Figures 15 and 16.

9. Conclusions

The RF power and voltage requirement for the SLS storage ring are quite modest and achievable with conventional, already well-proven equipment that can be available and operational within relatively short times. It is planned to use four 500 MHz plants, each consisting of a normal conducting single cell cavity of the ELETTRA type, powered with a 180 kW CW klystron amplifier via a WR1800 waveguide line. The cavity input coupler will be of the coaxial type, terminated by a coupling loop. For coping with the cavity HOM impedances, the parasitic frequencies will be detuned to avoid resonant excitations by the beam. This can be achieved by combining three tuning means: temperature control of the cooling water, elastic mechanical deformation and a plunger tuner. In addition, each plant will be equipped with standard amplitude and phase regulation loops.
In spite of the lower power requirement, one plant similar to those of the storage ring will be used for the booster with the intention of standardizing.
This system - while operating at relatively conservative performance levels - should be capable of fulfilling the SLS nominal requirement.
The use of superconducting cavities has been ruled out as a starting solution. However, for improving the beam lifetime the initial nc system could be further complemented with idle (no external power source) sc cavities. Such a system could be used either to double the fundamental RF voltage with one 500 MHz sc cavity, or to lengthen the bunches by a factor three to four with one (possibly two) 2nd or 3rd harmonic sc cavity(ies). Furthermore, we could cumulate the benefits of both methods in implementing three idle sc cavities: one 500 MHz and two harmonic cavities. This would theoretically result in improving the beam life time by about one order of magnitude and alternatively offer the possibility of shortening the bunches by a factor two. A more detailed description of such a *hybrid "powered nc and idle sc" system* is reported in [6]. In principle, it should not pose any special problem. On the contrary, it appears to be particularly flexible and easy to control; moreover, the difficulties related to the transmission of large power through the sc cavities and the associated technological problems are eliminated. The main challenge for the use of a sc cavity in such a

high current machine certainly resides in the damping of the parasitic HOM impedances which can drive coupled bunch instabilities. Programs of development aimed at solving this problem, have been launched in several laboratories [29-33]. We will attentively follow their advancement in view of a possible application in the SLS.

10. Acknowledgements

I would like to thank all the PSI members who contributed to the design and specification of the RF system, especially M. E. Busse-Grawitz and W. Tron for their active participation, as well as M. Rohrer for providing the drawings.

11. References

[1] P. Marchand, RF for Synchrotron Radiation Sources (1.5-2.5 GeV), SLS-Note 6/95, presented at the first RF Workshop of the New European Light Source Projects, Karlsruhe Research Center, October 1995.
[2] P. Marchand, RF system for the SLS, PSI SLS Note 14/96, September 1996.
[3] P. Marchand, Use of an idle superconducting cavity for improving the energy acceptance in the SLS storage ring, PSI SLS Note 19/96, October 1996.
[4] J. Bengtsson et al, Increasing the energy acceptance of high brightness synchrotron light storage ring, NIM A404, p. 237-247, 1998.
[5] P. Marchand, Foils of the SLS MAC meeting, December 1996 and Presentation at the 4th RF workshop of the New European Light Source Projects, Daresbury, UK, April 1997.
[6] P. Marchand, Possible upgrading of the SLS RF system for improving the beam lifetime, PSI Note SLS-TME-TA-1998-0012, September 1998.
[7] M. Böge et al, The Swiss Light Source Accelerator Complex: An Overview, presented at the EPAC98, Stockholm, June 1998.
[8] A. Fabris and M. Svandrlik, private communication.
[9] F. Perez, Comparative Study of Cavities for the LSB, LSB/RF/01/96, 01-05-96.
[10] P.A. McIntosh, Preliminary Investigations of an RF Cavity for Diamond, DIAMOND/RF/95/01, September 1995.
[11] H.O. Moser et al, Vorschlag zum Bau einer Synchrotronstrahlungsquelle (ANKA) im Forschungszentrum Karlsruhe zur Förderung der industriellen Umsetzung von Mikrofertigungs- und Analytikverfahren, Forschungszentrum Karlsruhe, September 1995.
[12] P. Marchand, Design of the RF accelerating system for the storage ring of the B-Meson Factory proposed at PSI, PSI-TM-12-89-04.
[13] A. Massarotti et al, 500 MHz Cavities for the Trieste Synchrotron Light Source ELETTRA, Proceedings of the EPAC90, Nice, France, p. 919-921, June 1990.
[14] A. Massarotti et al, The RF System of ELETTRA, Proceedings of the EPAC94, p. 1853-1855, London, June 1994.
[15] S. Voigt et al, Leistungstest der ELETTRA-Einkopplung, Versuchprotokoll PSP Nr : 1.0600, Forschungszentrum Karlsruhe, March 1997.
[16] THOMCAST AG, Brief Description of the Pulse-Step Modulator TSM 6, TSM6_E.PM5, September 1996.
[17] K. Robinson, CEA-II (1956) and CEAL 1010 (1964).
[18] A. Karantzoulis et al, Observation of Instabilities in the ELETTRA Storage Ring, Proceedings of the EPAC94, p. 119-121, London, June 1994.
[19] P. Marchand, The Collective Phenomena in the B-Meson Factory Storage Ring proposed at PSI, PSI-TM-12-89-05, July 1989.
[20] M. Zobov et al, Collective Effects and Impedance Study for the DAΦNE Φ-Factory, LNFN-95/041 (P), July 1995.

[21] H. Schwartz and R. Rimmer, RF System Design for the PEPII B-Factory, Proceedings of the EPAC94, p. 1882-1884, London, June 1994.
[22] T. Kageyama et al, Design of a Prototype of RF Cavity for the KEK B-Factory (KEKB), Proceedings of the EPAC94, p. 2098-2100, London, June 1994.
[23] P. Marchand, RF System for High Luminosity e+ e- Colliders, Proceedings of the EPAC90, p. 1088-1090, Nice, June 1990.
[24] M. Svandrlick et al, Improved Methods of Measuring and Curing Multibunch Instabilities in ELETTRA, presented at the EPAC96, Sitges, Spain, June 1996.
[25] A Wrulich et al, Observation of Coupled Bunch Instabilities in ELETTRA, presented at the EPAC96, Sitges, Spain, June 1996.
[26] M. Svandrlick et al, Simulations and Measurements of Higher Order Modes of the ELETTRA RF Cavities in view of Coupled Bunch Instability Compensation by Temperature Variation, presented at the EPAC96, Sitges, Spain, June 1996.
[27] SLS Design Handbook, Version 30. November 1996, section 2.7.
[28] C. Gough et al, The SLS Booster Synchrotron, presented at the EPAC98, Stockholm, June 1998.
[29] J. Kirchgessner, Review of the Development of RF Cavities for High Currents, Proceedings of the IEEE PAC, p. 1469-1473, Dallas, May 1995.
[30] T. Tajima et al, Development of HOM Damper for B-Factory (KEKB) Superconducting Cavities, Proceedings of the IEEE PAC, p. 1469-1473, Dallas, May 1995.
[31] W. Hartung et al, Measurement of the Interaction between a Beam and a Beam Line Higher-Order Mode Absorber in a Storage Ring, Proc. of the IEEE PAC, p. 3294-3296, Dallas, May 1995.
[32] A. Fabris et al, Design of a 3^{rd} harmonic superconducting cavity for bunch lengthening in ELETTRA, presented at the EPAC98, Stockholm, June 1998.
[33] A. Mosnier et al, HOM damping in SOLEIL superconducting cavity, presented at the EPAC98, Stockholm, June 1998.

Revolution frequency, f_o [MHz]	1.04	
Momentum compaction, α	7. E-4	
Beam current, I_b [A]	0.4	
Energy, E [GeV]	2.4	
Radiation loss / turn, ΔU [MeV]	0.6	
Momentum spread, σ_p [%]	0.09	
Longitudinal damping time τ_s [ms]	4.5	
Transverse damping times, $\tau_x \approx \tau_y$ [ms]	9.	
RF frequency, f_{RF} [MHz]	499.652	
Harmonic number, $h = f_{RF} / f_o$	480	
RF power into the beam, P_b [kW]	240.	
RF voltage, V_{RF} [MV]	2.0	2.6
Overvoltage, q	3.3	4.3
RF acceptance, ε_{RF} [%]	± 3.0	± 3.7
Bunch length, σ_s [mm]	4.4	3.8
Synchrotron frequency, f_s [kHz]	6.8	7.8
Synchrotron tune, $Q_s = f_s / f_o$ [E-3]	6.5	7.5
Synchronous phase, ϕ_s [degree]	17.5	13.3

Table 1: Basic parameters for the SLS storage ring.

Resonant frequency, f_r	499.652 MHz
Shunt impedance, R_s	3.4 MΩ
Quality factor, Q_o	40000
Accelerating RF voltage, V_{RF}	650 kV
Power dissipation, P_d	65 kW

Table 2 : Main cavity parameters.

I_b [mA]	V_{RF} [MV]	P_d (1c) [kW]	P_b (1c) [kW]	P_t (1c) [kW]	β_m	Δf_m [kHz]	nb of cav.
400.	2.0	37.	60.	97.	2.6	32.	4
400.	2.6	60.	60.	120.	2.0	27.	4
400.	2.0	65.	80.	145.	2.2	24.	3

Table 3 : SLS possible operating conditions with 4 or 3 (out of 4) cavities in use.

- V_{RF} is the accelerating voltage "seen" by the beam (transit time factor included);
- P_d (1c), P_b (1c) and P_t (1c): wall dissipation, power delivered to the beam and total RF power per cavity;
- β_m, Δf_m : optimum coupling factor and detuning (zero reflected power at full beam current).

Frequency	499.652 MHz
1dB bandwidth (minimum)	± 1 MHz
RF nominal output power	> 180 kW
RF operating power	150 kW
Efficiency at 150 kW	> 60%
Tolerable load VSWR (all phases) at 180 kW	> 1.3
Duty cycle	cw
Output power dynamic	35 dB
Harmonic content	< - 30 dBc
Spurious and sideband level	< - 60 dBc
Signal to noise ratio within bandwidth	> 60 dB
Saturated drive power at 150 kW	< 25 W
Continuous collector dissipation capability	> 300 kW
RF phase variation vs. output power for full drive modulation	< 20°
RF phase variation over beam voltage variation for fixed modulation anode voltage	< 10°/ 1%
Variation of RF output power over beam voltage in saturated drive	< 0.1 dB / 1%
RF phase variation over cathode current	< 12° / A
Klystron input VSWR	< 1.5
Maximum RF radiation	0.1 mW/cm²
Maximum X-ray emission	0.1 μSv/h
Max. permissible energy in HV breakdown	35 J
Cathode potential for 150 kW output power	< 42 kV
Maximum operational cathode voltage	46 kV
Maximum modulating anode current	5 mA

Table 4 : Main klystron characteristics and performance.

Parameter	*Specification*	*Note*
Voltage	0 - 46 kV	negative voltage
Current	0 - 7.5 A	
Efficiency	> 97%	
Voltage accuracy (better than)	1%	
Voltage ripple (less than)	1% pp 75 V rms 15 V rms 3 V rms 50 V rms	overall 1 kHz to 2 kHz 2 kHz to 4 kHz 4 kHz to 12 kHz above 12 kHz
Speed	1 ms	
Voltage overshoot	< 5%	under any load condition
Energy into klystron arc	< 15 J	max. 70 V arc voltage
Input voltage	400 V ± 5%	3-phase 50 Hz
Tolerable mains 3-phase asymmetries	5%	voltage drop on one line

Table 5 : Main specifications for the klystron DC supply.

HOM	f_m (48 °C) [MHz]	R/Q [Ω]	Q	R_s [kΩ]	τ_m [kHz/°C]	φ_m
L1	949.506	28.8	35300	1017	- 11.5	0.63
L2	1057.199	0.7	33700	24	-19.3	-0.31
L3	1421.456	5.0	39300	197	-43.1	-2.16
L4	1514.638	4.9	17400	85	-28.2	-0.31
L5	1606.348	9.1	18100	165	-41.6	-2.33
L6	1876.971	0.3	41100	12	-33.4	-0.14
L7	1948.475	1.8	33100	60	-51.2	-2.23
L8	2072.036	0.1	12500	1	-110.9	-8.94
L9	2124.792	7.7	27000	208	-111.4	-9.3

Table 6 : Measured longitudinal HOM parameters of the ELETTRA cavity [26];
τ_m is the HOM frequency temperature dependence with the fundamental mode frequency kept constant by mechanical deformation;
φ_m is the ratio of HOM - to - fundamental frequency variation.

HOM	f_m (48 °C) [MHz]	$(R/Q)_T$ [Ω/m]	Q	R_T [kΩ/m]	τ_m [kHz/°C]	φ_m
T1H	743.169	72.5	40000	2.9	-36.3	-3.1
T1V	743.303	72.7	39900	2.9	-36.0	-3.1
T2H	745.280	246.5	35300	8.7	-13.5	0.0
T2V	746.463	245.9	36200	8.9	11.5	0.0
T3H	1114.274	301.9	37100	11.2	-18.5	0.2
T3V	1114.706	304.2	35500	10.8	-16.1	0.5
T4H	1241.307	118.0	17800	2.1	-49.7	-4.0
T4V	1242.237	118.0	17800	2.1	-49.7	-3.9
T5H	1304.432	8.6	23200	0.2	-38.9	-2.3

Table 7 : Measured transverse HOM parameters of the ELETTRA cavity [26];
τ_m and φ_m are defined as in Table 6;
TiH / TiV correspond to the horizontal / vertical polarizations for dipole mode i.

repetition rate	3	Hz
beam current	12	mA
injection energy	100	MeV
final energy	2.4	GeV
revolution frequency	1.11	MHz
RF frequency	500	MHz
harmonic number	450	
Number of cavities	1	
shunt impedance Rs	3.4	MΩ
At final energy		
RF voltage	0.5	MV
cavity dissipation	36	kW
radiation loss/turn	240	keV/turn
RF power into beam	3	kW
RF acceptance *	± 0.46	%
bunch length (rms)	19	mm
synchrotron frequency	8.2	kHz

Table 8 : Main parameters of the SLS booster.
(* 2.5 % at injection)

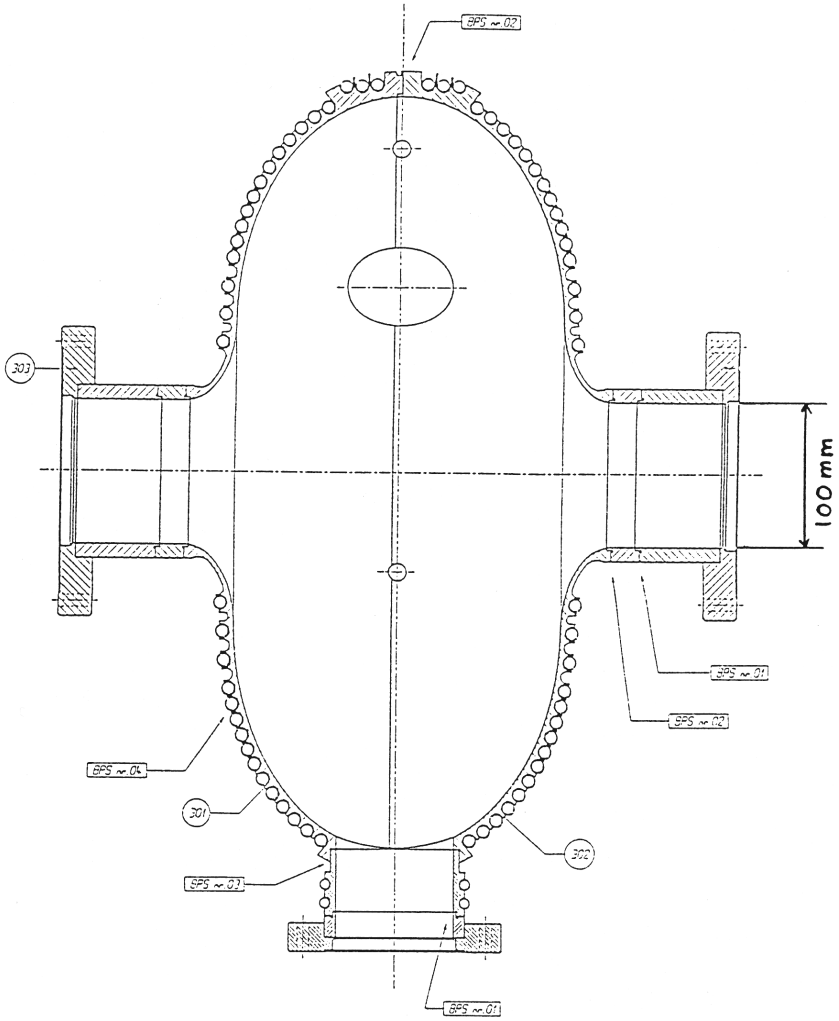

Figure 1 : Cross section of the ELETTRA cavity.

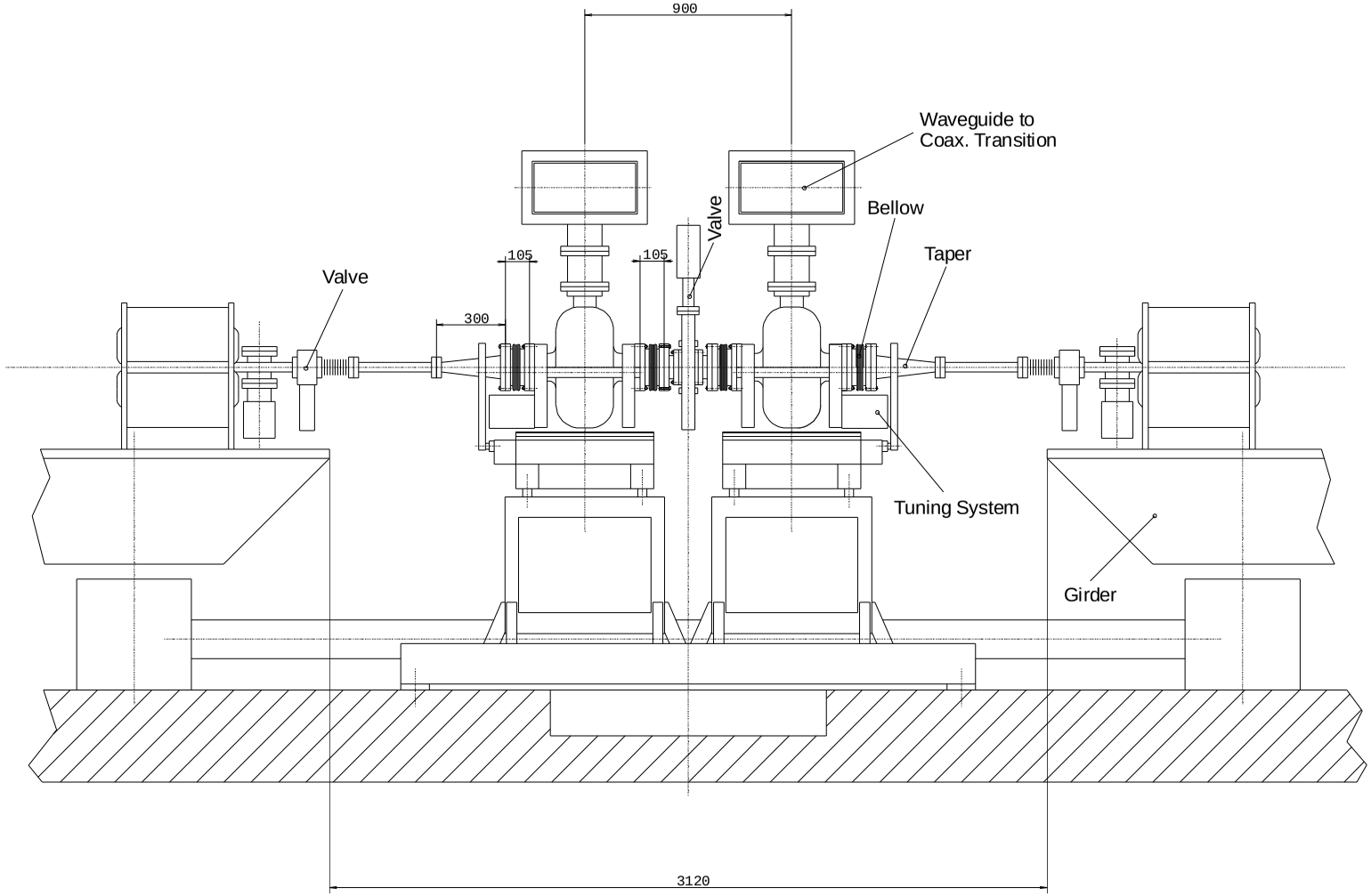

Figure 2 : Cavity layout in the storage ring.

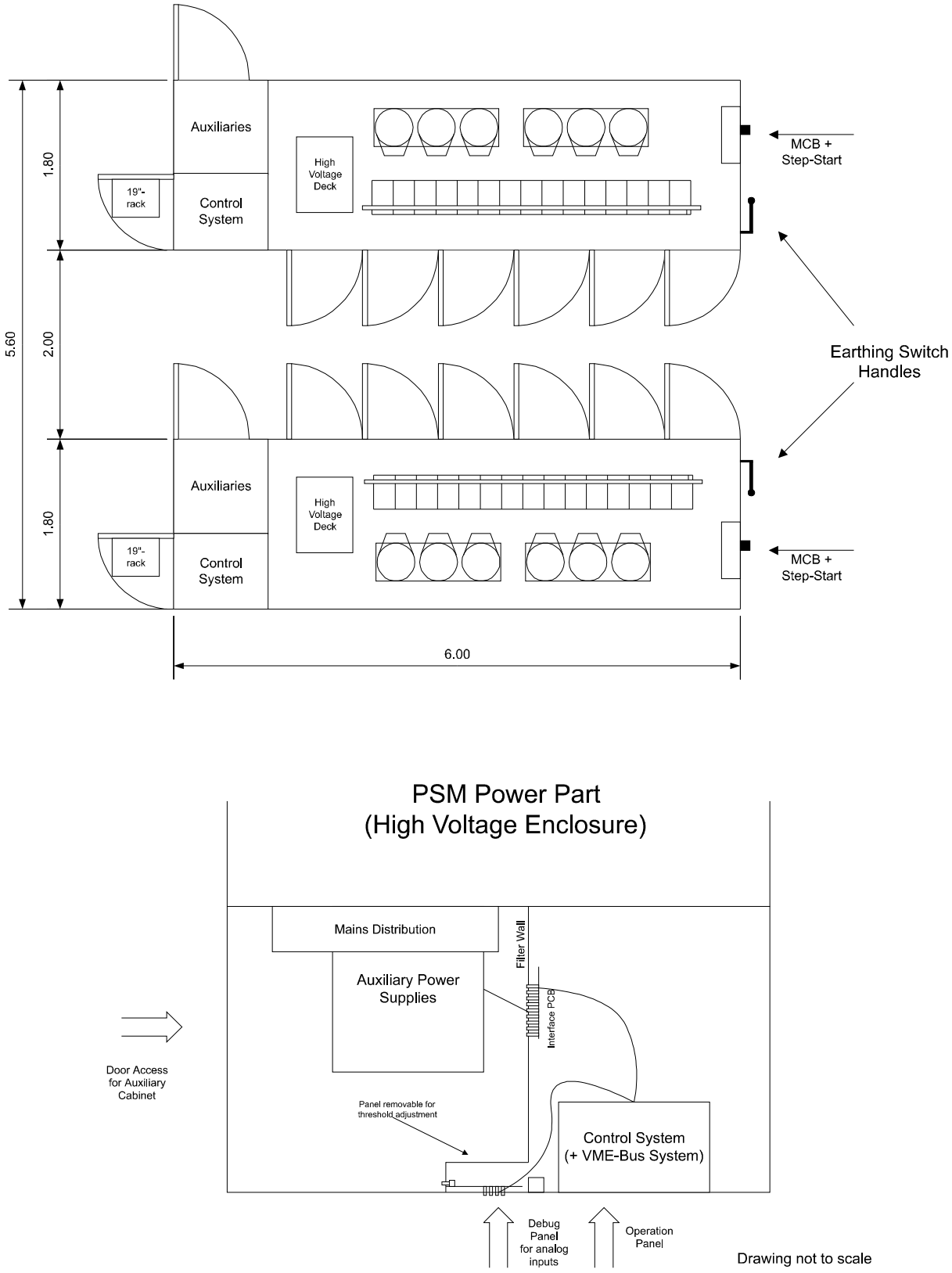

Figure 3 : Power supply and control system cabinets.

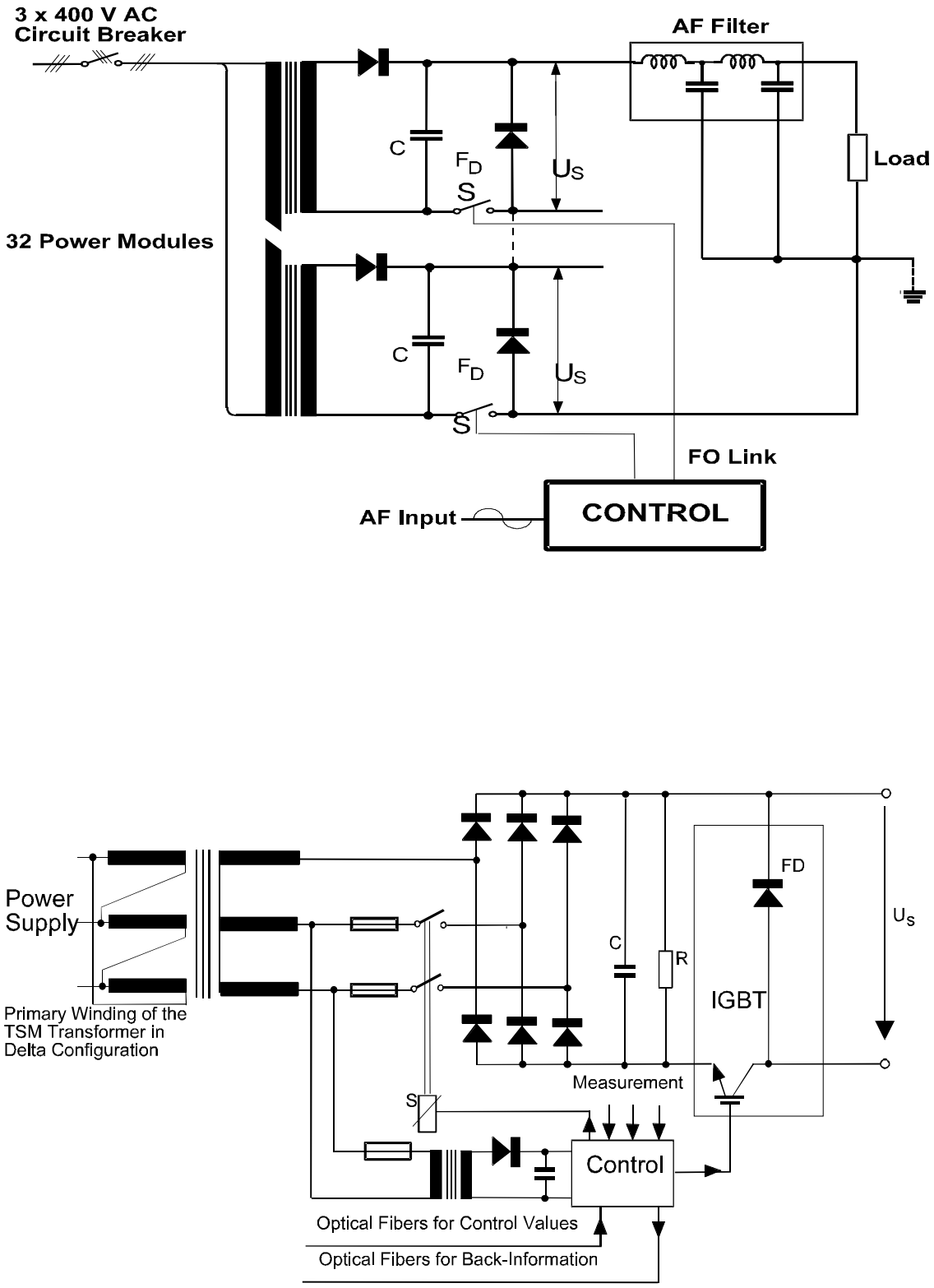

Figure 4 : Conceptual electronic diagrams of the klystron high voltage power supply (Pulse Step Modulator from THOMCAST AG).

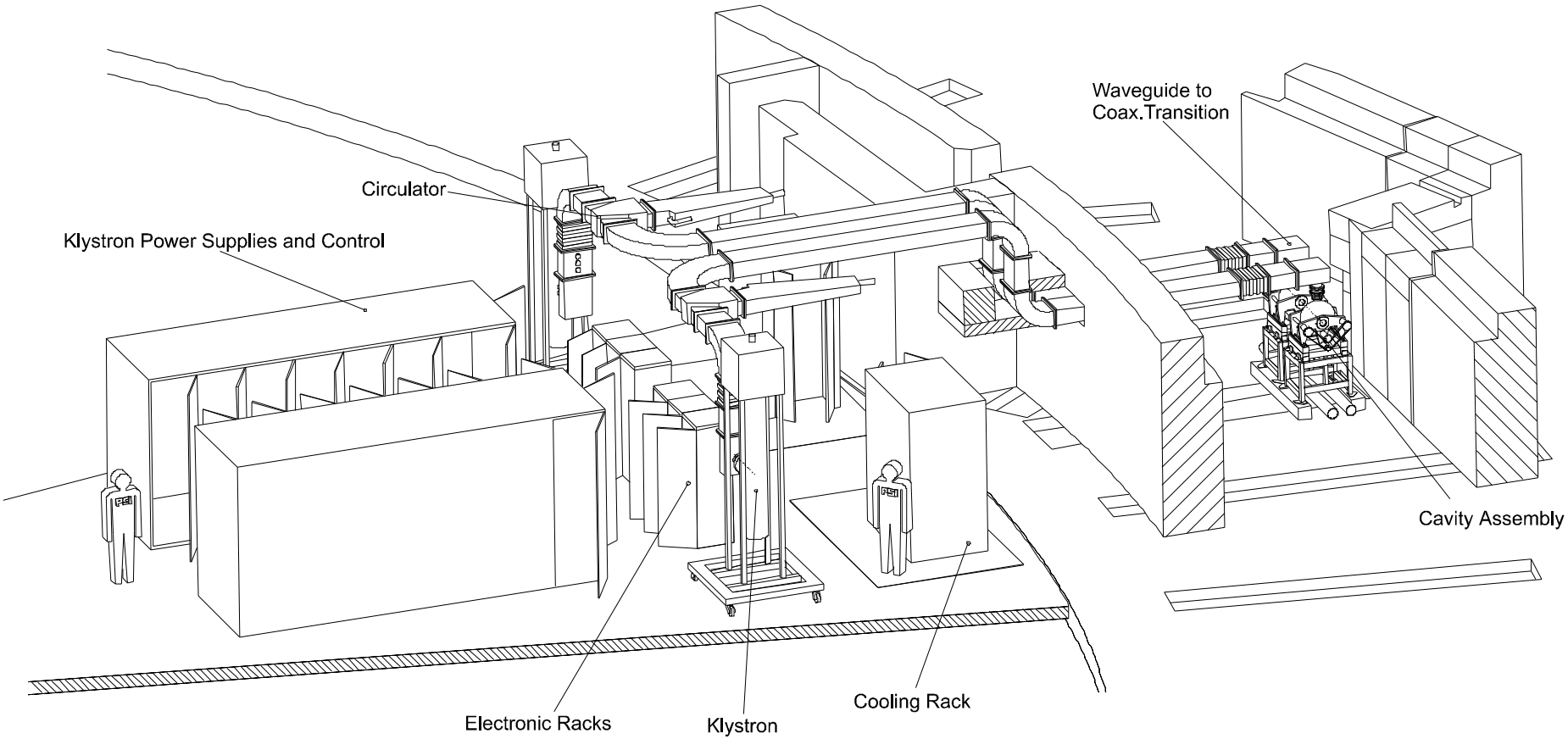

Figure 5 : Storage ring RF station.

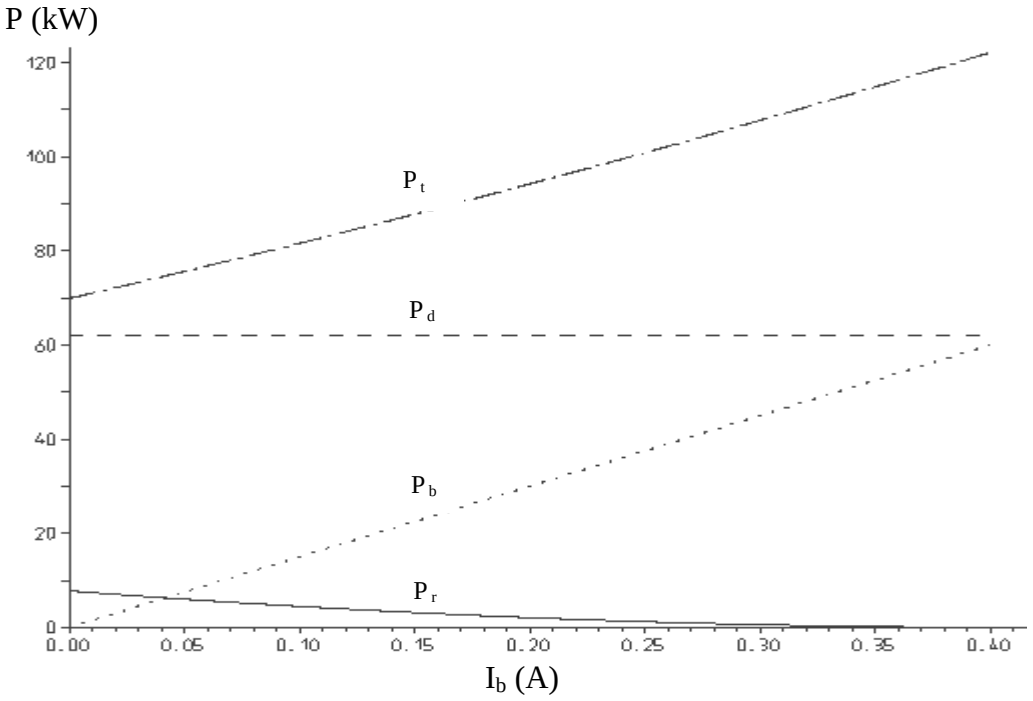

Figure 6 : Wall dissipation (P_d), power delivered to the beam (P_b), reflected power (P_r) and total power (P_t) for one of the four SLS storage ring cavities during injection at 2.4 GeV (V_{RF} = 2.6 MV, β = 2).

$$P_t = \frac{(1+\beta)^2}{4\beta} P_d \left(1 + \frac{P_b}{P_d (1+\beta)} \right)^2 ;$$

$$P_r = P_t - (P_b + P_d) .$$

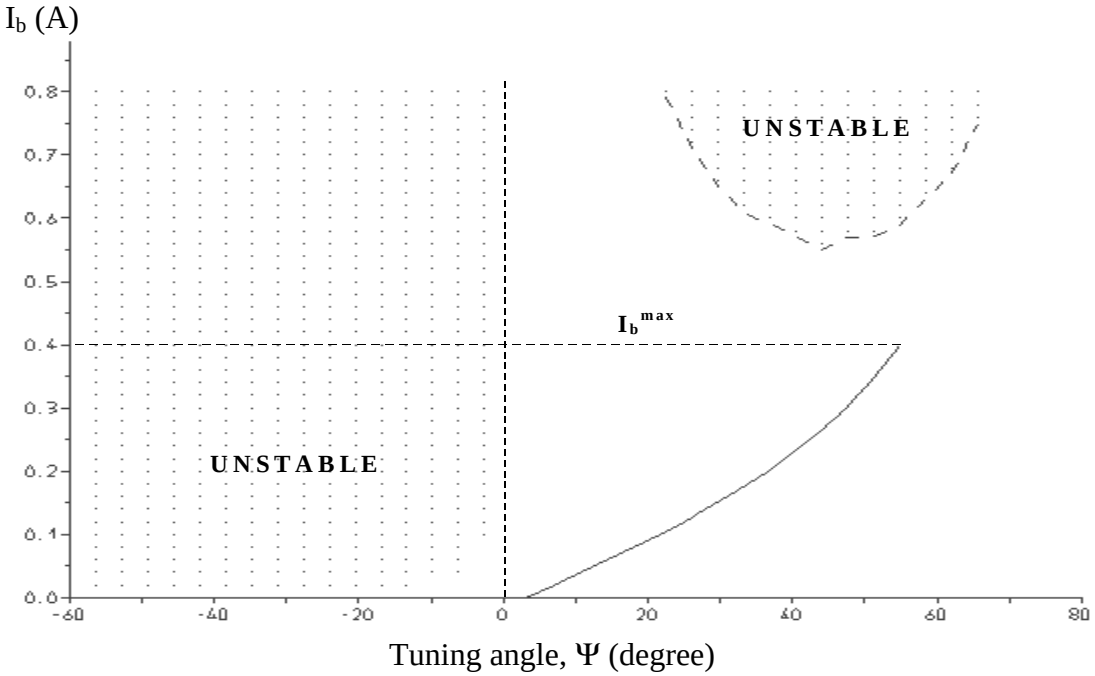

Figure 7 : Robinson's stability diagram for the same conditions as above.

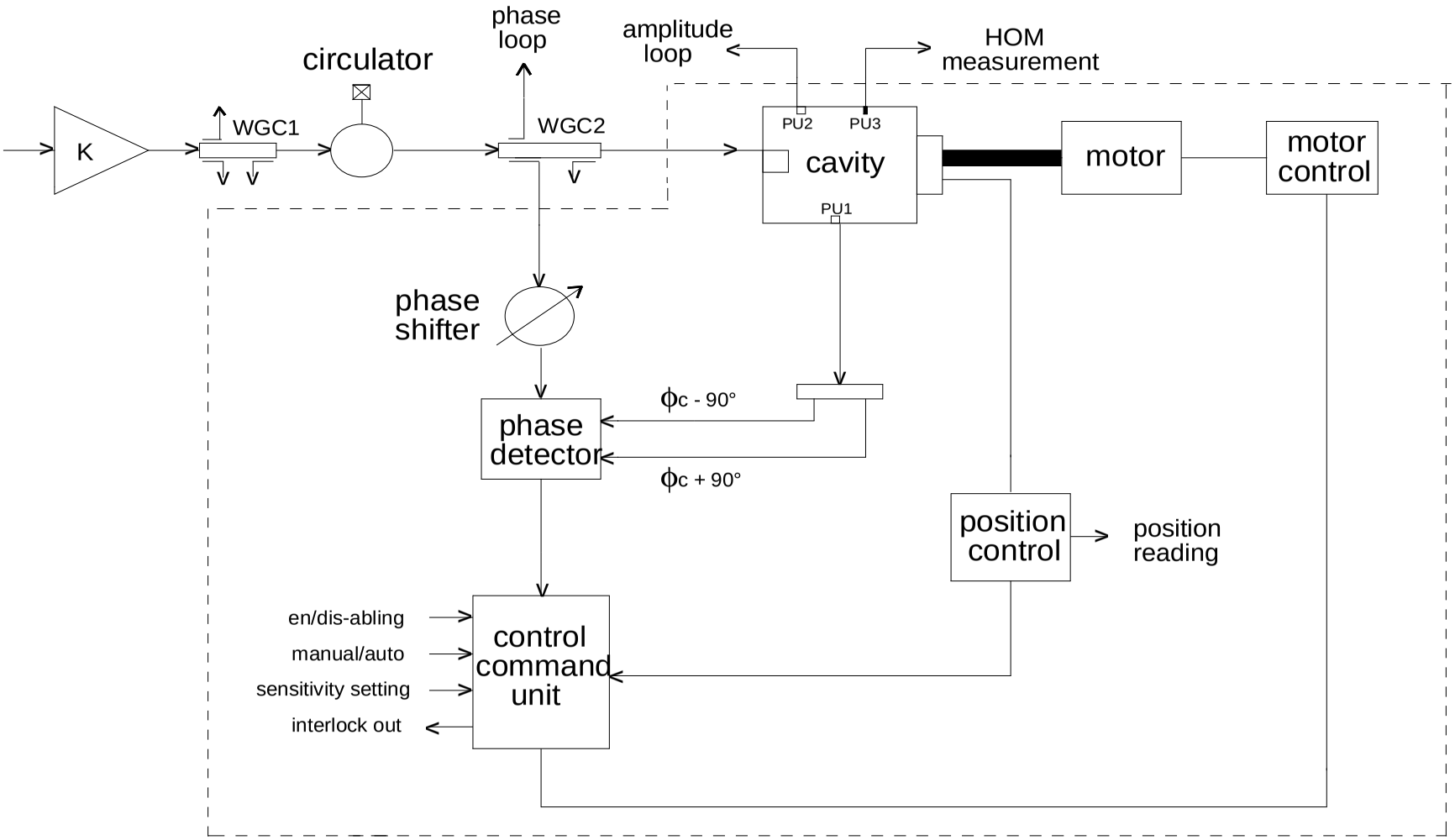

Figure 8 : Block diagram of the frequency tuning loop.

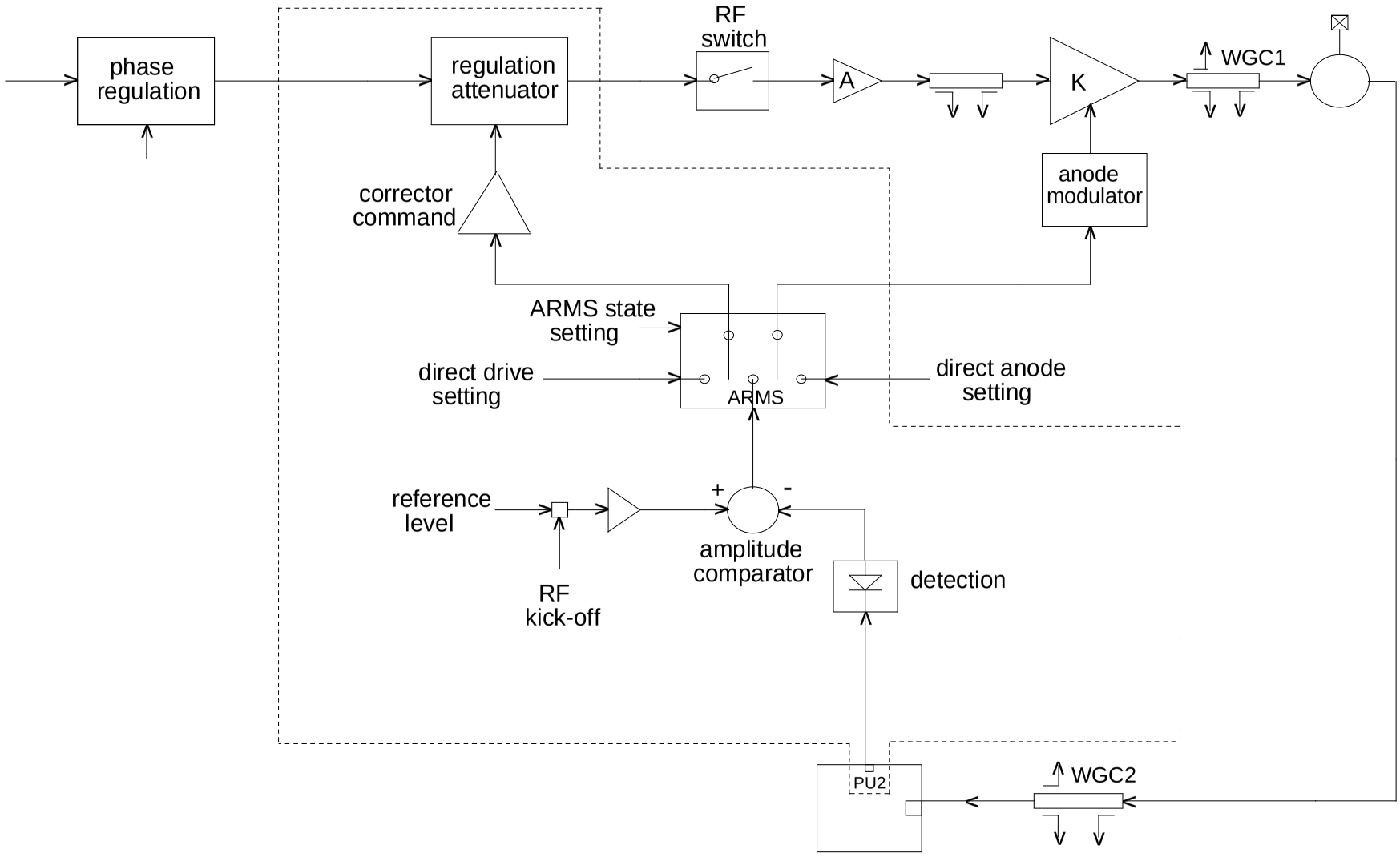

Figure 9 : Block diagram of the amplitude loop (ARMS: Amplitude Regulation Mode Switch).

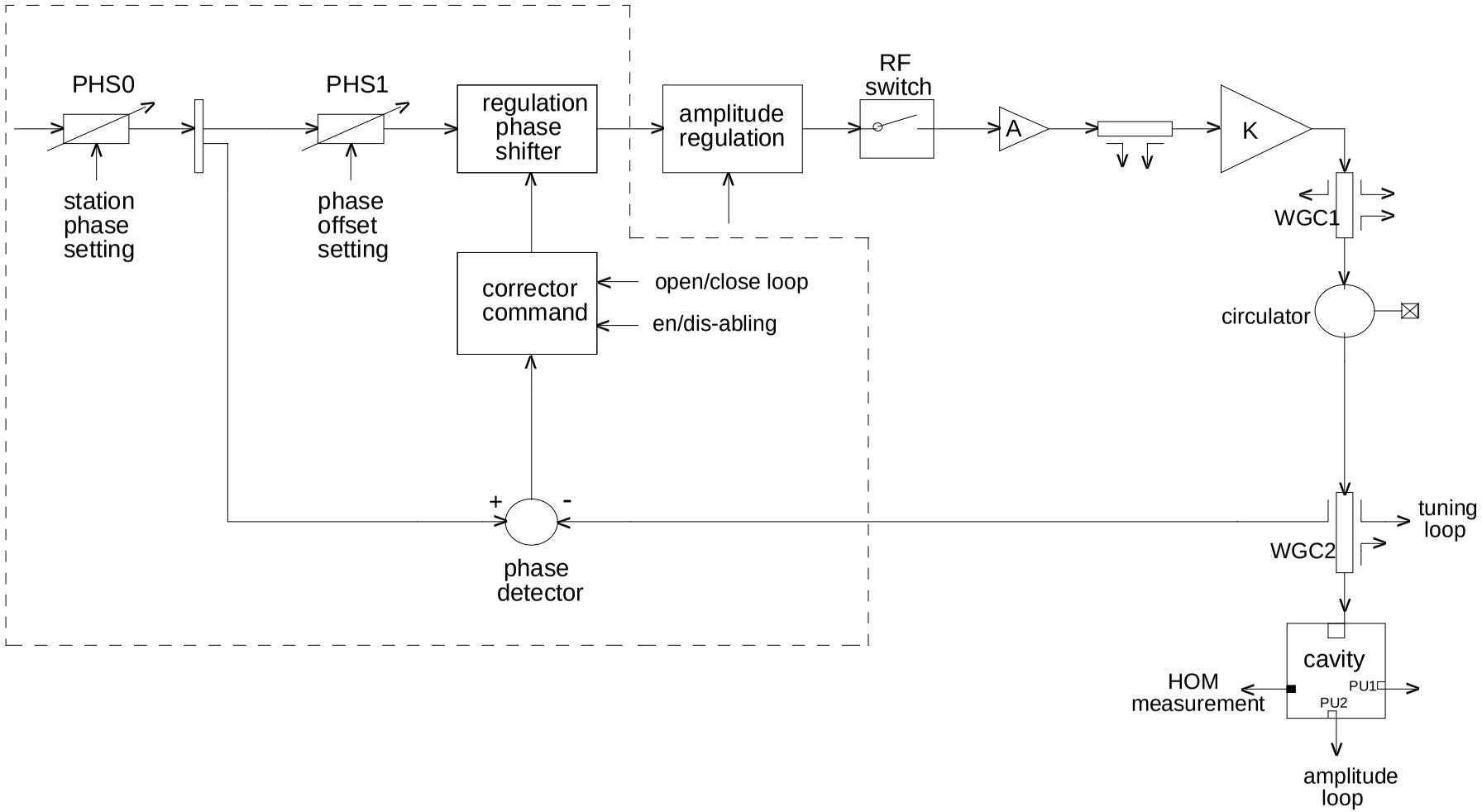

Figure 10 : Block diagram of the phase loop.

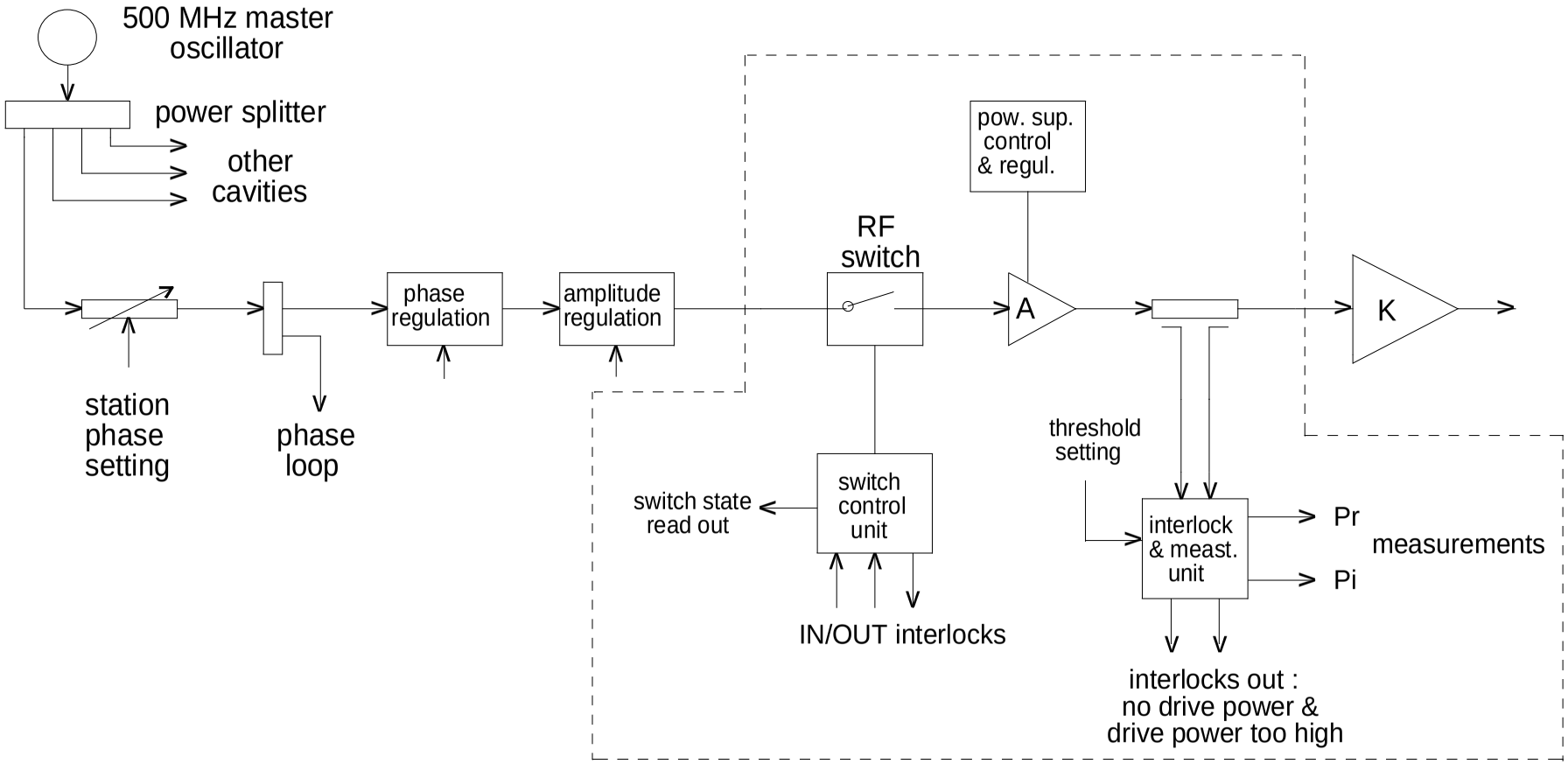

Figure 11 : Block diagram of the drive chain.

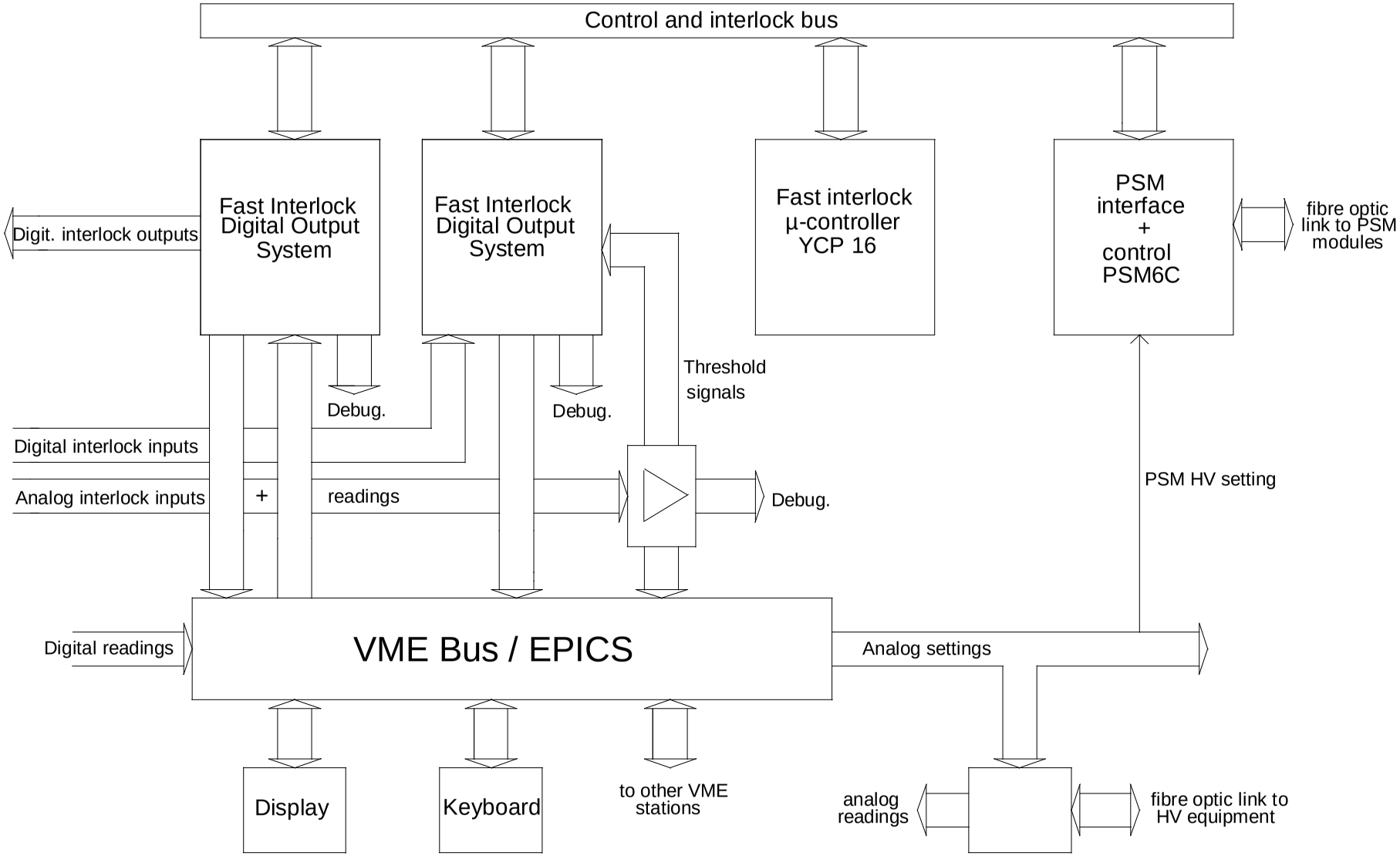

Figure 12 : Block diagram of the RF control system.

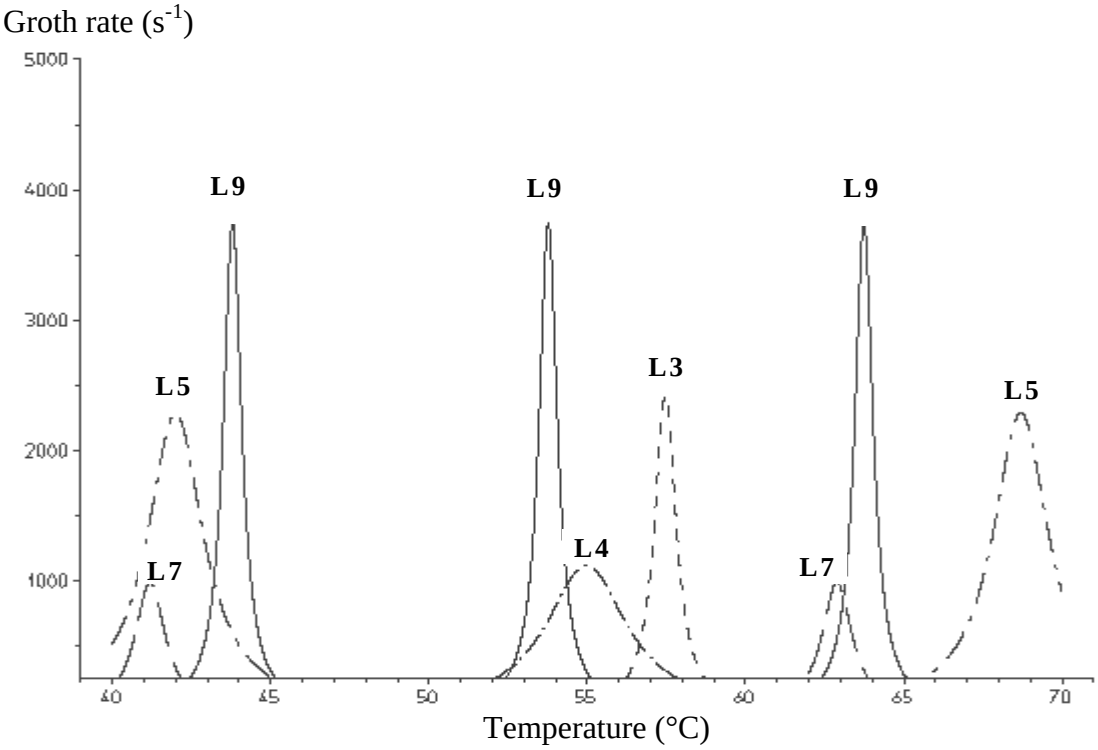

Figure 13: Growth rates of the longitudinal CBI versus cavity temperature (HOM parameters from Table 6).

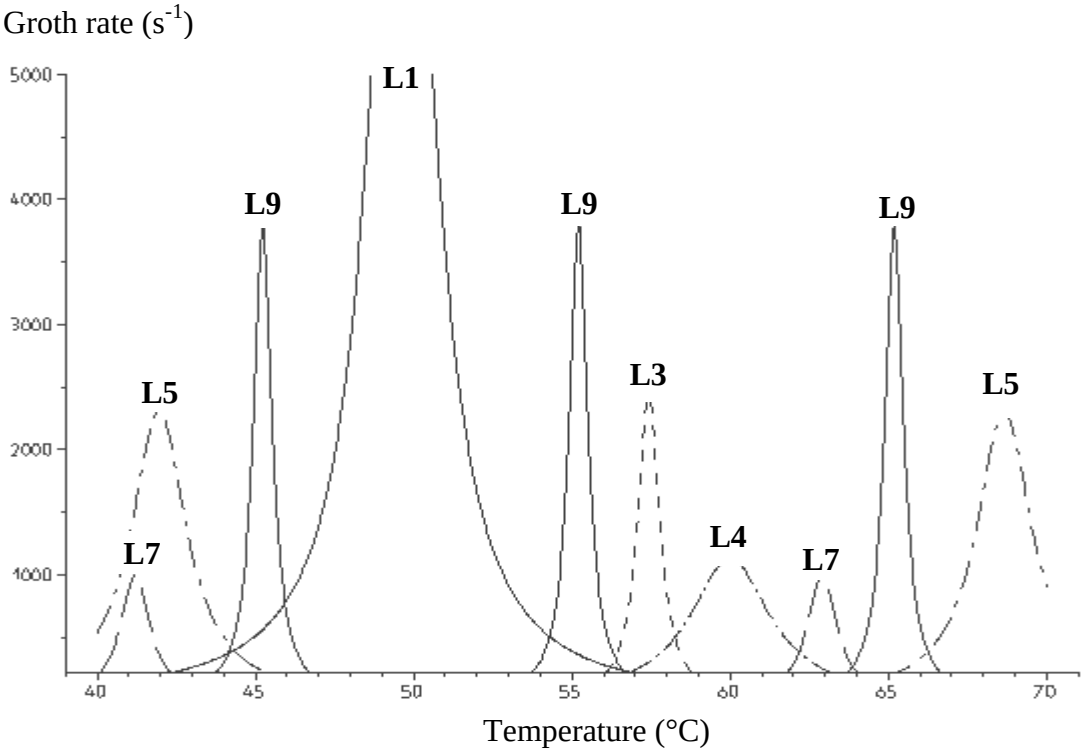

Figure 14: As above, but the HOM frequencies have been artificially set such that to simulate the most unfavourable case.

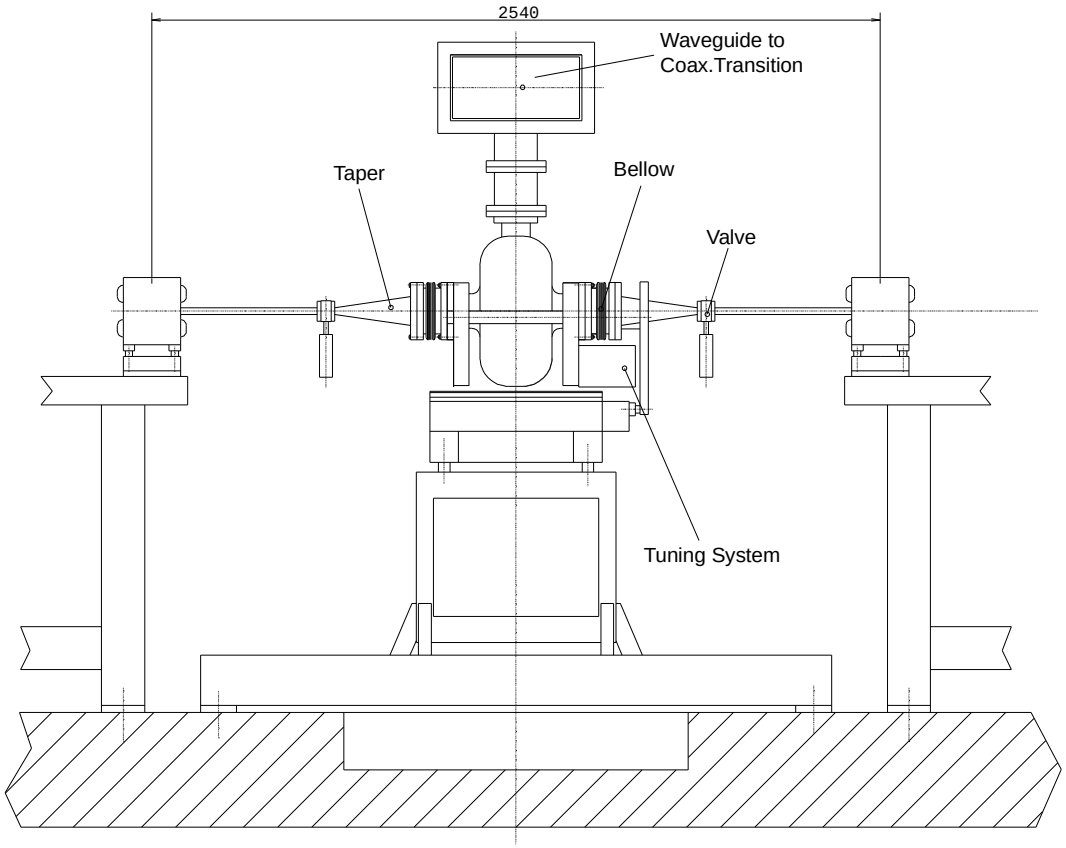

Figure 15 : Booster cavity layout.

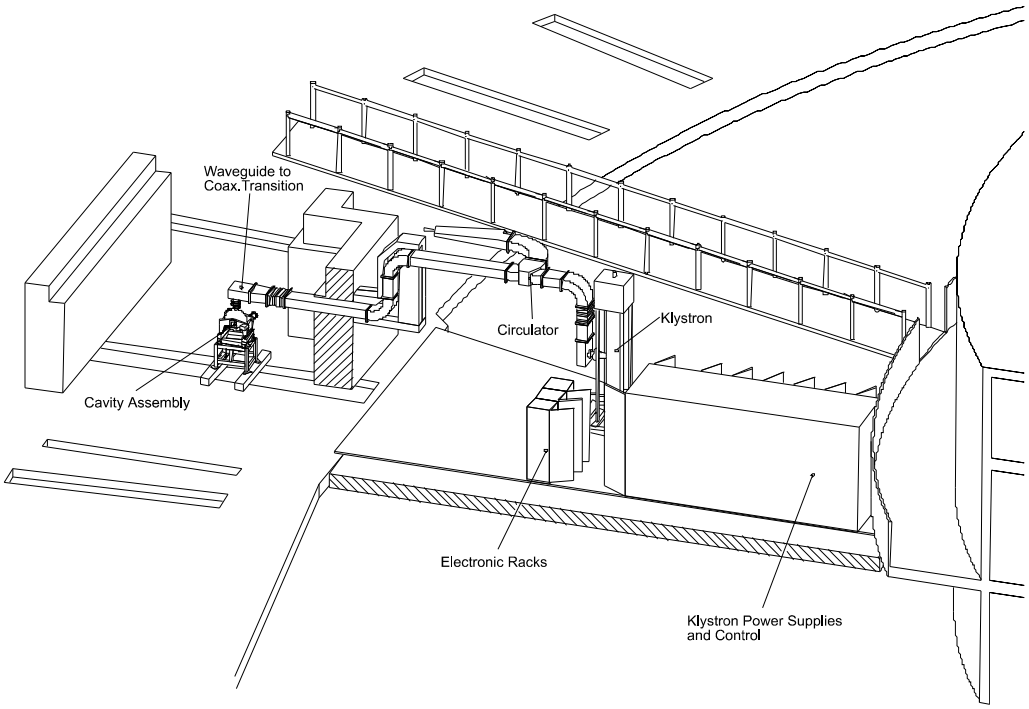

Figure 16 : Booster RF station.